Article

Cell Reports

Reversal of Defective Mitochondrial Biogenesis in Limb-Girdle Muscular Dystrophy 2D by Independent Modulation of Histone and PGC-1α Acetylation

Graphical Abstract

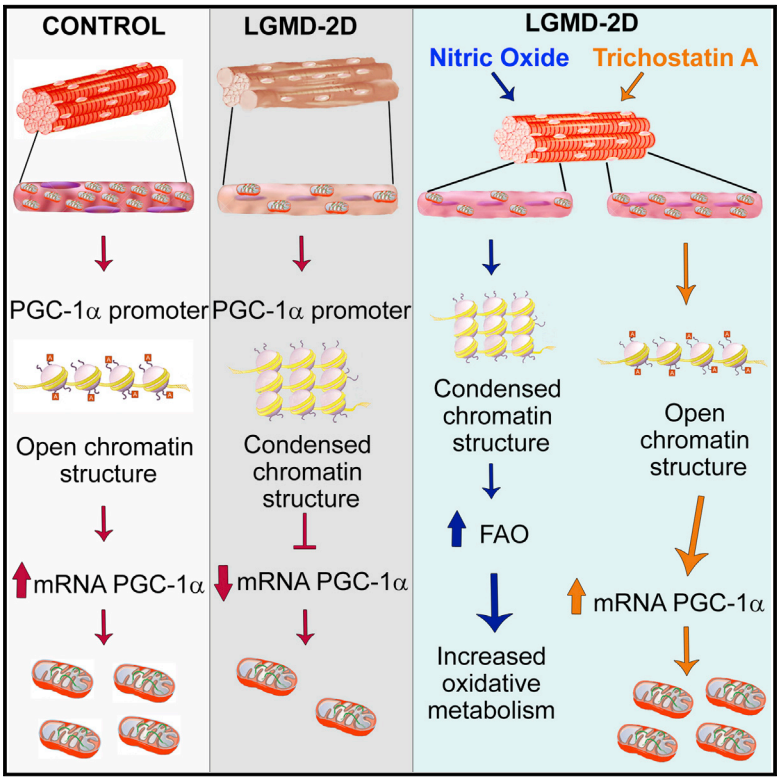

Highlights

- LGMD-2D patients and α-SG null mice display reduced mitochondrial content
- Reduced acetylation of the PGC-1α promoter causes the mitochondrial defect
- Trichostatin A reverses chromatin modifications, restoring mitochondrial biogenesis
- Nitric oxide activates a salvage pathway that shunts faulty mitochondrial biogenesis

Authors

Sarah Pambianco, Matteo Giovarelli, Cristiana Perrotta, ..., Lucia Latella, Emilio Clementi, Clara De Palma

Correspondence

emilio.clementi@unimi.it (E.C.), clara.depalma@unimi.it (C.D.P.)

In Brief

Pambianco et al. describe a specific mitochondrial defect in LGMD-2D, characterized by reduced mitochondrial number. This defect is due to impaired mitochondrial biogenesis associated with condensed chromatin at the PGC-1α promoter and is reversed by Trichostatin A. Nitric oxide rescues the bioenergetics defect without affecting mitochondrial biogenesis.

Pambianco et al., 2016, Cell Reports *17*, 3010–3023
December 13, 2016
http://dx.doi.org/10.1016/j.celrep.2016.11.044

CellPress

OPEN ACCESS
CellPress

Cell Reports
Article

Reversal of Defective Mitochondrial Biogenesis in Limb-Girdle Muscular Dystrophy 2D by Independent Modulation of Histone and PGC-1α Acetylation

Sarah Pambianco,[1,9] Matteo Giovarelli,[1,9] Cristiana Perrotta,[1] Silvia Zecchini,[2] Davide Cervia,[1,3] Ilaria Di Renzo,[1] Claudia Moscheni,[1] Michela Ripolone,[4] Raffaella Violano,[4] Maurizio Moggio,[4] Maria Teresa Bassi,[5] Pier Lorenzo Puri,[6,7] Lucia Latella,[6,8] Emilio Clementi,[2,5,*] and Clara De Palma[2,10,*]

[1]Department of Biomedical and Clinical Sciences "Luigi Sacco," Università degli Studi di Milano, 20157 Milano, Italy
[2]Department of Biomedical and Clinical Sciences, Unit of Clinical Pharmacology, University Hospital "Luigi Sacco"-ASST Fatebenefratelli Sacco, National Research Council-Institute of Neuroscience, Università degli Studi di Milano, 20157 Milano, Italy
[3]Department for Innovation in Biological, Agro-food and Forest systems, Università degli Studi della Tuscia, 01100 Viterbo, Italy
[4]Neuromuscular Unit, Dino Ferrari Centre, IRCCS Foundation Ca' Granda Ospedale Maggiore Policlinico, Università degli Studi di Milano, 20122 Milano, Italy
[5]IRCCS Eugenio Medea, 23842 Bosisio Parini, Italy
[6]Epigenetics and Regenerative Pharmacology, IRCCS Fondazione Santa Lucia, 00142 Roma, Italy
[7]Sanford Children's Health Research Center, Sanford Prebys Burnham Medical Discovery Institute, La Jolla, CA 92037, USA
[8]National Research Council-Institute of Translational Pharmacology, 00179 Roma, Italy
[9]Co-first author
[10]Lead Contact
*Correspondence: emilio.clementi@unimi.it (E.C.), clara.depalma@unimi.it (C.D.P.)
http://dx.doi.org/10.1016/j.celrep.2016.11.044

SUMMARY

Mitochondrial dysfunction occurs in many muscle degenerative disorders. Here, we demonstrate that mitochondrial biogenesis was impaired in limb-girdle muscular dystrophy (LGMD) 2D patients and mice and was associated with impaired OxPhos capacity. Two distinct approaches that modulated histones or peroxisome proliferator-activated receptor-gamma coactivator 1 α (PGC-1α) acetylation exerted equivalent functional effects by targeting different mitochondrial pathways (mitochondrial biogenesis or fatty acid oxidation[FAO]). The histone deacetylase inhibitor Trichostatin A (TSA) changed chromatin assembly at the PGC-1α promoter, restored mitochondrial biogenesis, and enhanced muscle oxidative capacity. Conversely, nitric oxide (NO) triggered post translation modifications of PGC-1α and induced FAO, recovering the bioenergetics impairment of muscles but shunting the defective mitochondrial biogenesis. In conclusion, a transcriptional blockade of mitochondrial biogenesis occurred in LGMD-2D and could be recovered by TSA changing chromatin conformation, or it could be overcome by NO activating a mitochondrial salvage pathway.

INTRODUCTION

Mitochondrial defects accompany several forms of muscular dystrophies, genetic diseases characterized by progressive skeletal muscle wasting, local inflammation, and compensatory regeneration (Barton et al., 2005; Kornegay et al., 2014; Ruegg, 2013). While loss of functional dystrophin protein is the primary cause of Duchenne muscular dystrophy (DMD), other pathogenic events have recently been associated with DMD, including decreased mitochondrial mass (Godin et al., 2012) and reduced expression of enzymes involved in glycolytic and oxidative metabolism (Guevel et al., 2011; Percival et al., 2013; Rybalka et al., 2014). Likewise, in limb-girdle muscular dystrophy 2D (LGMD-2D), loss of α sarcoglycan (α-SG), an essential component of the dystrophin-glycoprotein complex, is accompanied with reduced transcription of nuclear-encoded mitochondrial genes similar to that observed in DMD (Chen et al., 2000; Pescatori et al., 2007). This evidence indicates that metabolic dysregulation is a pathogenic event shared by muscular dystrophies in which deficiency of a component of the dystrophin-associated complex can impair signaling to the mitochondria.

An important aspect in dystrophic skeletal muscle including LGMD-2D (Crosbie et al., 2002) is the displacement of the muscle-specific variant of the enzyme neuronal nitric oxide (NO) synthase (nNOSμ), usually localized at the sarcolemma in close contact with the sarcoglycan-dystroglycan complex, with reduced generation of NO. NO in skeletal muscle regulates metabolism and energy expenditure, coupling energy demand and supply through a variety of actions (De Palma and Clementi, 2012; Stamler and Meissner, 2001). In addition, NO stimulates mitochondrial biogenesis (Nisoli et al., 2003, 2007), regulates mitochondrial dynamics (De Palma et al., 2010), and contributes to muscle physiological growth and repair via several actions including inhibition of histone deacetylases (HDACs) (Colussi et al., 2008, 2009; Tidball and Wehling-Henricks, 2014). Normalization of NO production slows disease progression in mouse

models of muscular dystrophies and it is currently investigated in therapeutic perspective (Brunelli et al., 2007; D'Angelo et al., 2012; Sciorati et al., 2010).

Here, we characterize the mitochondrial dysfunction in LGMD-2D patients and in the α-SG mouse model of the disorder, showing a defective OxPhos capacity, accompanied by persistent impairment of mitochondrial biogenesis that could not be reactivated by physiological mitochondrial biogenetic stimuli such as cold. These defects coincided with formation of pathogenic chromatin modifications at the peroxisome proliferator-activated receptor-gamma coactivator 1 α (PGC-1α) promoter that could be reversed using the deacetylase inhibitor Trichostatin A (TSA), restoring mitochondrial biogenesis and enhancing muscle oxidative capacity. By using the NO donor molsidomine, we identify a physiological pathway that can rescue functionally the bioenergetic defects of dystrophic muscles by shunting the defective mitochondrial biogenesis. We describe a network whereby the activation of SIRT1 causes the deacetylation of PGC-1α ultimately leading to promotion of fatty acid oxidation and a shift toward more oxidative muscle fibers. Thus, two distinct therapeutic approaches yield similar functional effects targeting different mitochondrial pathways.

RESULTS

Muscles of LGMD-2D Patients Show Altered Mitochondrial Content and Activity

We found a reduction of mitochondrial DNA (mtDNA) in muscle biopsies from LGMD-2D patients as compared to healthy age-matched controls (Figure 1A), associated with reduced expression of the PGC-1α mRNA, the master regulator of mitochondrial biogenesis (Lin et al., 2005), and its downstream target, nuclear respiratory factor 1 (NRF1) (Figure 1B) as well as reduced citrate synthase (CS) activity (Figure 1C).

In LGMD-2D muscle sections, we also found, with respect to healthy controls, reduced cytochrome *c* oxidase (COX) activity and succinate dehydrogenase staining (SDH), used as good proxies for mitochondrial activity (Figures 1D and 1E). Altogether, these data indicate that mitochondrial number and function in muscles of LGMD-2D patients are defective.

Muscles of α-SG Null Mice Show Altered Mitochondrial Content and Activity

To investigate the mechanism of altered mitochondrial function in LGMD-2D we relied on the α-SG null mouse model of the disease. We analyzed diaphragm and tibialis anterior (TA) muscles of 5-month-old α-SG null mice compared to age-matched wild-type (WT) mice as controls. We found a marked reduction of mtDNA (Figures 2A and S1A) as well as of genes encoding different electron transport chain subunits, namely cytochrome *b* (CYT B), ATPase, and COX subunit IV (COX IV) (Figures 2B and S1B). Consistently, the protein levels of COX IV and two other mitochondrial proteins, porin (VDAC-1) and cytochrome *c* oxidase subunit I (mtCO1), were lower in α-SG null than in control mice (Figure 2C). The analysis of mitochondrial ultrastructure by electron microscopy showed a reduction of mitochondrial density in α-SG null mice (Figure 2D), in agreement with decreased CS activity (Figure 2E).

To evaluate mitochondrial function, the respiratory rates expressed per tissue wet weight were assessed in saponin-permeabilized muscle fibers. As shown in Figures 2F and S1C, the glutamate-malate-induced respiration (state 2) was significantly reduced in α-SG null diaphragm versus control; further, in both α-SG null diaphragm and TA, the ADP-driven glutamate-malate respiration (state 3) was defective, and this impairment persisted after the consecutive addition of succinate alone (state 3 + Succ) or succinate plus rotenone (state 3 + Succ + Rot). These data indicate a deficiency of the entire respiratory chain in α-SG null mice, rather than damage to a specific complex. The differences in mitochondrial activity appreciated with fibers analysis were no longer observed when the respiratory rates were assessed by comparing equal amounts of mitochondria isolated from α-SG null and control skeletal muscles (Figure 2G). This indicates that existing mitochondria have normal respiratory activity, and the bioenergetics defect of α-SG null fibers resides in the reduced mitochondrial content.

Of note, this mitochondrial defect was restricted to skeletal muscle fibers and correlated to the disease stage, as other tissues/organs such as liver, heart, and brown adipose tissue (BAT) from α-SG null and control animals did not show differences in mtDNA content (Figure S1D). Similar results were obtained in *mdx* mice, the mouse model of DMD, thus indicating that the mitochondrial defect occurs selectively in skeletal muscles and is associated with sarcolemmal instability (i.e., perturbation of the dystrophin-sarcoglycan complex) (Figures S1E and S1F).

Mitochondrial Biogenesis Is Impaired in Muscle of α-SG Null Mice

The number of mitochondria is known to increase during muscle growth (Laker et al., 2012). We found that in WT mice, mtDNA was unchanged between 1.5 and 3 months, while it increased significantly between 3 and 5 months, in both diaphragm and TA (Figures 3A and S2A). Consistently, we found increased PGC-1α mRNA levels in WT at 5 months when compared to 1.5-month-old mice (Figure 3B). In contrast, in α-SG null muscles, we did not observe any increase in mitochondrial mass (Figures 3A and S2A) nor in PGC-1α mRNA levels (Figure 3B) during postnatal life, however, at 5 months, both PGC-1α mRNA (Figure 3B and S2B) and proteins (Figure 3C) levels were significantly lower in dystrophic mice than in controls.

Furthermore, the mRNA levels of NRF-1 and mitochondrial transcription factor A (TFAM), were significantly reduced in α-SG null mice (Figures 3D and S2B). These results suggest that postnatally α-SG null muscles are unable to increase mitochondrial mass because the mitochondrial biogenesis pathway is impaired.

PGC-1α is also known to slow calcium handling in skeletal muscle (Summermatter et al., 2012); we found that α-SG null muscles showed upregulation of calcium-signaling molecules, such as calcium release-activated calcium modulator 1 (ORAI1) and stromal interaction molecule 1 (STIM1) (Figure S2C). Thus, the possibility that altered PGC-1α levels could influence mitochondrial calcium homeostasis in LGMD-2D and that this may further contribute to the mitochondrial bioenergetics defect cannot be excluded.

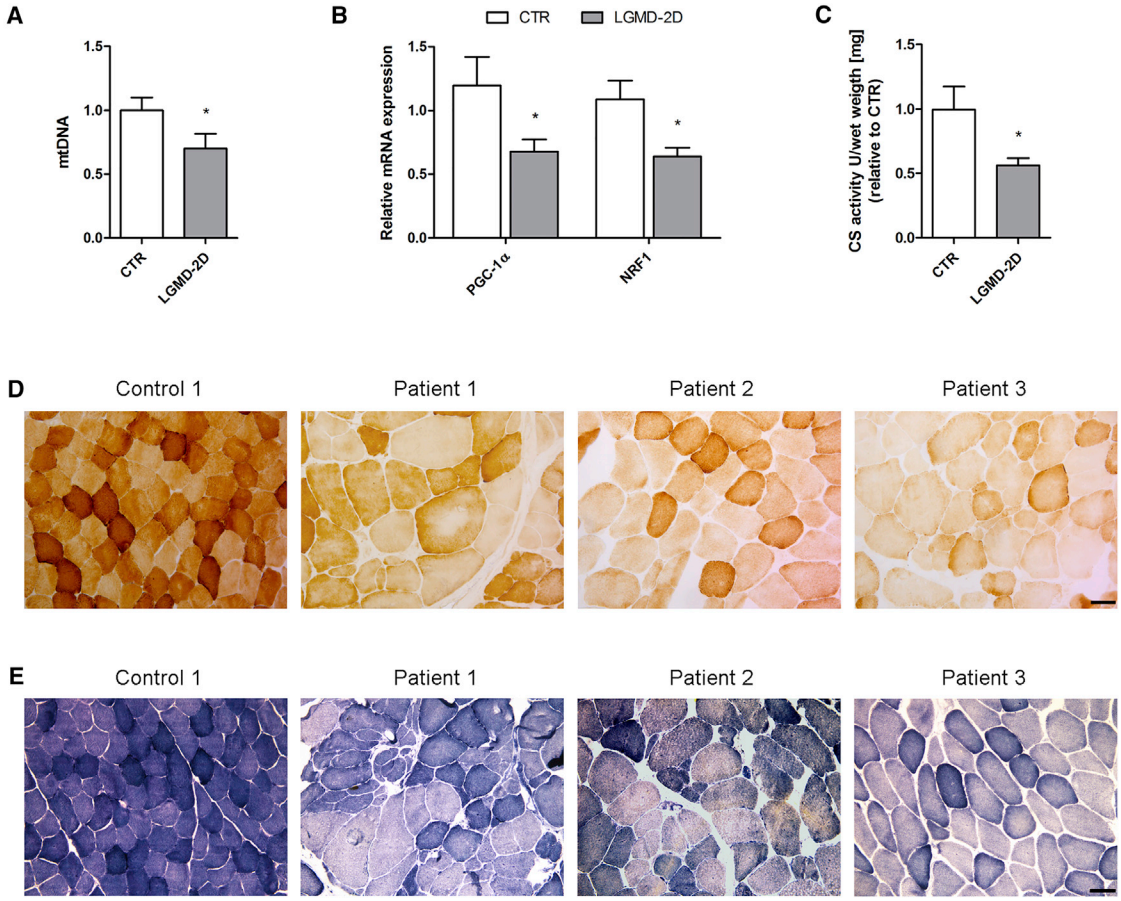

Figure 1. Muscles of LGMD-2D Patients Show Altered Mitochondrial Content and Activity

Analysis of bicep muscles of patients compared to control subjects.

(A) Analysis of mtDNA content (n = 9 for LGMD-2D patients and n = 10 for control subjects).

(B) Quantitative real-time PCR analysis of mitochondrial biogenesis genes (PGC-1α and NRF1) (n = 9 for LGMD-2D patients and n = 10 for control subjects).

(C) CS activity (n = 5 for LGMD-2D patients and n = 7 for controls subjects).

(D and E) Representative COX (D) and SDH (E) staining of muscle cryosections of one control and three LGMD-2D patients. Scale bar, 100 μm.

Values are expressed as mean ± SEM. *Versus control (*$p < 0.05$).

We next directly assessed whether mitochondrial biogenesis was altered by evaluating the response to cold exposure, a classical mitochondrial biogenetic stimulus (Hock and Kralli, 2009). Cold exposure increased the mRNA levels of PGC-1α and NRF1, and mitochondrial content in muscles of WT mice, but not in α-SG null mice (Figures 3E and 3F, S2D, and S2E). These data indicate that α-SG null muscles display a persistent defect in mitochondrial biogenesis that accounts for a reduced mitochondrial content.

Muscles of α-SG Null Mice Show Epigenetic Modifications on PGC-1α Promoter

We investigated the molecular determinants of the impaired PGC-1α expression and mitochondrial biogenesis in α-SG null mice. Dynamic chromatin modifications regulate PGC-1α expression and hence the oxidative capacity of skeletal muscles in pathological conditions, such as diabetes (Galmozzi et al., 2013). We used chromatin immunoprecipitation analysis (ChIP) to analyze three regulatory histone modifications at PGC-1α locus (Figure 4A). Specifically, we used antibodies that recognize marks of active or repressed promoters, namely lysine 4 (Lys4), methylation (H3K4me3), and lysine 27 (Lys27) methylation (H3K27me3), respectively. No significant changes were observed in H3K4me3 and H3K27me3 either in WT controls or dystrophic mice (Figure S3). This evidence suggests that PGC-1α promoter adopts a bivalent chromatin conformation that poises for signal-dependent activation, as previously described for "developmentally" regulated genes (Azuara et al., 2006; Bernstein et al., 2006; Mikkelsen et al., 2007). We assessed whether the signal that resolves such a bivalency at the PGC-1α promoter could be an increase in histone H3 acetylation. Indeed, increased H3 acetylation was observed in diaphragms from 5-month-old WT control mice, but not in α-SG null mice, in two different regions that map 430 bp upstream to the transcription start site (TSS) and CRE site (Figure 4B). These data indicate that the impairment of mitochondrial biogenesis in α-SG null mice is accompanied by a chromatin conformation of the PGC-1α promoter predictive of gene repression.

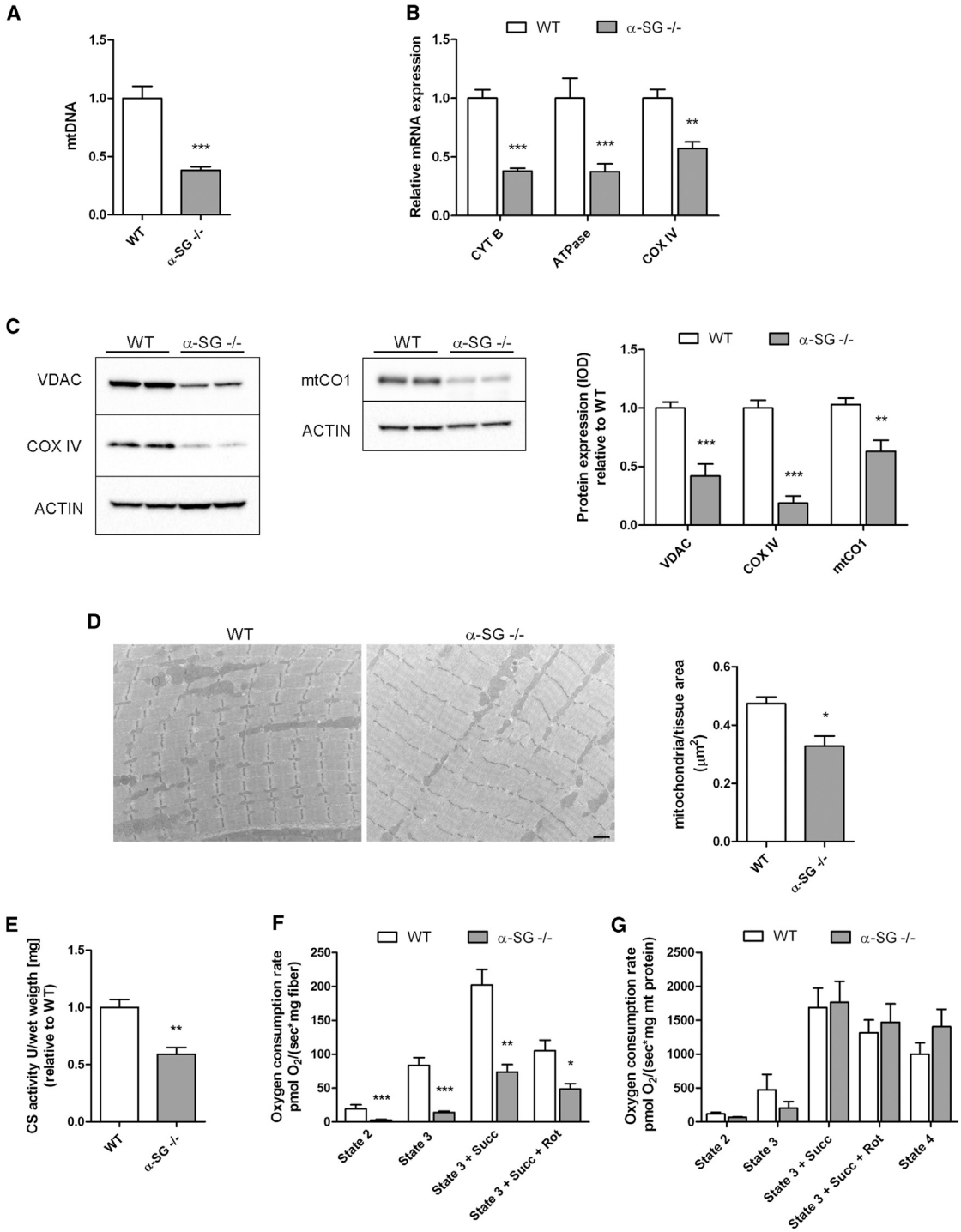

Figure 2. α-SG Null Mice Muscles Show Altered Mitochondrial Content and Activity

Analysis of a diaphragm of a 5-month-old α-SG null (−/−) compared to age-matched wild-type (n) mice.

(A) Analysis of mtDNA content (n ≥ 12 per genotype).

(B) Quantitative real-time PCR analysis of genes encoding electron transport chain subunits (n ≥ 5 per genotype).

(C) Immunoblot of VDAC, COX IV, mtCO1, and Actin (n ≥ 6 per genotype). Densitometric quantification is provided.

(D) Electron microscopy analysis. Representative images are provided (n ≥ 4 per genotype). Histogram represents the quantification of the mitochondrial density calculated as number of mitochondria per tissue area. Scale bar, 1 μm.

(legend continued on next page)

To determine whether this epigenetic modification, that is associated with defects in mitochondrial biogenesis in α-SG null mice, could be pharmacologically reversed, we used the pan-HDAC inhibitor (HDACi) Trichostatin A (TSA) (Consalvi et al., 2013; Minetti et al., 2006). Increased histone acetylation, which reflects the bioactivity of deacetylase inhibitors, was evaluated in the PGC-1α promoter at 430 bp upstream to the TSS and CRE site. In both sites, acetylation levels were increased by TSA treatment (Figure 4C). Consistently, PGC-1α mRNA and protein levels (Figures 4D and 4E), as well as PGC-1α targets genes (Figure 4F), were significantly enhanced after TSA administration, indicating the reactivation of the gene expression program leading to mitochondrial biogenesis. Consequently, the mitochondrial mass was boosted by TSA treatment as indicated by the higher levels of mtCO1, and this resulted in a great improvement of diaphragm oxidative capacity, as detected by SDH and COX staining (Figures 4G–4I).

We and others have previously shown that nitric oxide (NO) mediates a functional link between dystrophin and HDAC2 (Cacchiarelli et al., 2010; Colussi et al., 2008). Because NO has mitochondrial biogenetic properties (Lira et al., 2010; Ventura-Clapier et al., 2008), we investigated whether NO delivery could reverse the impaired mitochondrial biogenesis by upregulating PGC-1α through promoter hyperacetylation. To this purpose, we used the NO donor molsidomine, which can be incorporated into the diet and delivered chronically in mouse models of muscular dystrophy (Buono et al., 2012; Cordani et al., 2014). Treatment for 4 months preserved skeletal muscle integrity, reduced fibrotic tissue, and decreased inflammatory infiltrate (Figure S4A) in agreement with studies that also demonstrate a functional recovery of spontaneous and forced motor activities (Buono et al., 2012; Zordan et al., 2013).

Surprisingly, molsidomine did not modify H3 acetylation of PGC-1α promoter at 430 bp upstream to TSS and CRE site in α-SG null diaphragm (Figure 5A). Likewise, PGC-1α mRNA levels (Figure 5B), as well as the expression of PGC-1α target genes (Figure S4B) and the mitochondrial density (Figures 5C), did not change after molsidomine treatment. The protein analysis confirmed the unchanged levels of PGC-1α and mitochondrial markers after molsidomine treatment (Figure 5D). These observations were not exclusive to the diaphragm as similar results were obtained in TA of α-SG null mice (Figures S4C and S4D) and clearly indicate that, at variance with *mdx* mice, chronic administration of NO, supplemented with the diet, does not target the pathogenic chromatin conformation of α-SG null mice and does not enhance mitochondrial biogenesis.

NO Improves Mitochondrial Function in the Absence of Mitochondrial Biogenesis

Despite the absence of mitochondrial biogenesis, the respiratory capacity of muscle fibers from diaphragm and TA of molsidomine-treated α-SG null mice was significantly enhanced (Figures 5E and S4E). Consistently, the production of OxPhos ATP by mitochondria isolated from α-SG null diaphragm treated with molsidomine was significantly higher than in untreated α-SG null muscles (Figure S4F). Thus, NO improved mitochondrial respiratory capacity while not increasing mitochondrial density.

Because improved OxPhos capacity can result in the variations of glycolytic and oxidative muscle fiber proportions (Feige et al., 2008), we evaluated whether NO promoted fiber-type switching. To this end, the contractile phenotype of α-SG null and WT mice was assessed by immunofluorescence of type I and IIa myosin heavy chains (MyHCs), both markers of slow-twitch fibers. α-SG null diaphragm displayed reduced expression of MyHC IIa, but not MyHC I, compared to WT and molsidomine-restored MyHC IIa levels (Figure 5F). Levels of MyHC IIa were increased by molsidomine in TA as well (Figure S4G). Consistently, SDH staining revealed that the proportion of blue-stained oxidative fibers in TA was higher in molsidomine-treated α-SG null mice than in untreated α-SG null mice (Figure S4H).

Molsidomine treatment increased the expression of medium- and long-chain acyl-CoA dehydrogenases (MCAD and LCAD, respectively) and pyruvate dehydrogenase kinase 4 (PDK4) in both the diaphragm and TA of α-SG null mice (Figures 5G and S5A). By contrast, the expression of genes controlling glycolysis, Krebs cycle, and mitochondrial function were not affected by molsidomine treatment (Figure S5B). Thus, the fiber switch induced by NO was associated with an increased expression of genes promoting the use of fatty acid over glucose (i.e., enzymes decreasing the utilization of pyruvate and increasing the flux of fatty acid in the muscle). Consistently, in myotubes, NO improved palmitate oxidation (Figure 5H) without affecting mitochondrial content and myogenic differentiation (Figure S5C).

Because SIRT1 is a key regulator of lipolysis and FAO (Gerhart-Hines et al., 2007), we assessed whether it can be modulated by NO. In diaphragm of α-SG null mice, molsidomine significantly enhanced SIRT1 mRNA expression (Figure 6A) resulting in decreasing acetylated levels of PGC-1α protein, a known substrate of SIRT1 (Figure 6B). The acetylation status of PGC-1α is considered a marker of SIRT1 activity in vivo because PGC-1α activity is described to be positively regulated by SIRT1-mediated deacetylation (Lagouge et al., 2006; Rodgers et al., 2005). However, NAD^+ is a rate limiting co-substrate for SIRT1, and altered NAD^+ levels in α-SG null muscle might affect SIRT1 activity. As shown in Figure 6C, NAD^+ levels were increased in the diaphragm of α-SG null mice, thus indicating that NAD^+ was not a limiting factor to SIRT-1 activity in dystrophic muscle. Treatment with molsidomine resulted in mild reduction of NAD^+ levels, probably caused by increased consumption, suggesting that NO stimulation of SIRT1 was independent of NAD^+ levels.

(E) CS activity ($n \geq 4$ per genotype).
(F) Mitochondrial respiration in permeabilized diaphragm muscle fibers ($n \geq 5$ per genotype).
(G) Mitochondrial respiration from isolated diaphragm mitochondria (n = 8 per genotype).
Values are expressed as mean ± SEM. *Versus WT (*$p < 0.05$, **$p < 0.01$, ***$p < 0.001$). See also Figure S1.

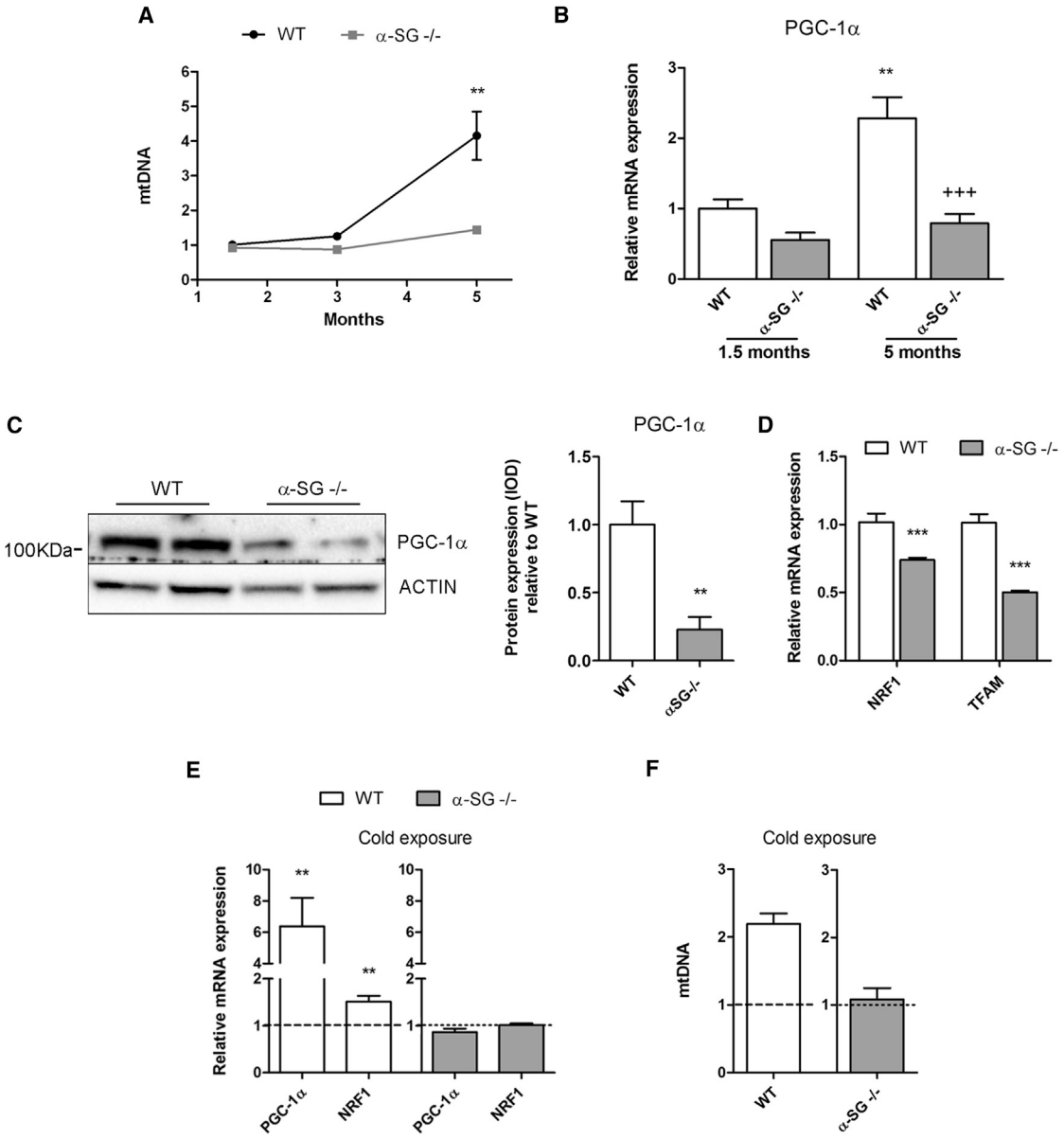

Figure 3. α-SG Null Mice Exhibit a Persistent Inhibition of Mitochondrial Biogenesis Process

(A) Analysis of mtDNA content in diaphragm of WT and α-SG$^{-/-}$ mice during postnatal life (1.5, 3, and 5 months of age). Values are expressed as mean ± SEM ($n \geq 3$ per group). *Versus each time point. (**$p < 0.01$).

(B) Quantitative real-time PCR analysis of PGC-1α in diaphragm of WT and α-SG$^{-/-}$ mice during postnatal life (1.5 and 5 months of age) ($n \geq 4$ per group). *Versus WT at 1.5 months of age (**$p < 0.01$); $^{+}$versus WT at 5 months of age ($^{+++}p < 0.001$).

(C) Immunoblot of PGC-1α and actin (n = 4 per genotype). Densitometric quantification is provided. *Versus WT (**$p < 0.01$).

(D) Quantitative real-time PCR analysis of NRF1 and TFAM in diaphragm of 5-month-old WT and α-SG$^{-/-}$ mice ($n \geq 3$). * versus WT (***$p < 0.001$).

(E and F) Quantitative real-time PCR analysis of mitochondrial biogenesis genes after 24 hr (E) and mtDNA content in diaphragm after 72 hr (F) of cold exposure (4°C) in diaphragm of 5-month-old WT and α-SG$^{-/-}$ mice relative to corresponding unstimulated controls ($n \geq 3$–4). *Versus unstimulated controls (dashed line, WT mice; dotted line, α-SG$^{-/-}$ mice) (**$p < 0.01$).Values are expressed as mean ± SEM. See also Figure S2.

SIRT1 activators enhance metabolic processes associated with low energetic status through AMPK activation (Chen and Guarente, 2007; Feige et al., 2008). In myotubes, short-term exposition to NO did not activate AMPK (Figure S6A); however, in dystrophic mice, molsidomine increased phosphorylation of AMPK and expression of the AMPK target, FOXO3a, (Figures 6D and 6E), supporting the idea that NO changes the metabolic status of dystrophic muscle and indirectly activates AMPK.

These effects of molsidomine were not restricted to diaphragm as similar data on SIRT1 expression levels, PGC-1α acetylation, and AMPK phosphorylation were also detected in TA muscle in response to molsidomine treatment (Figures S6B–S6D).

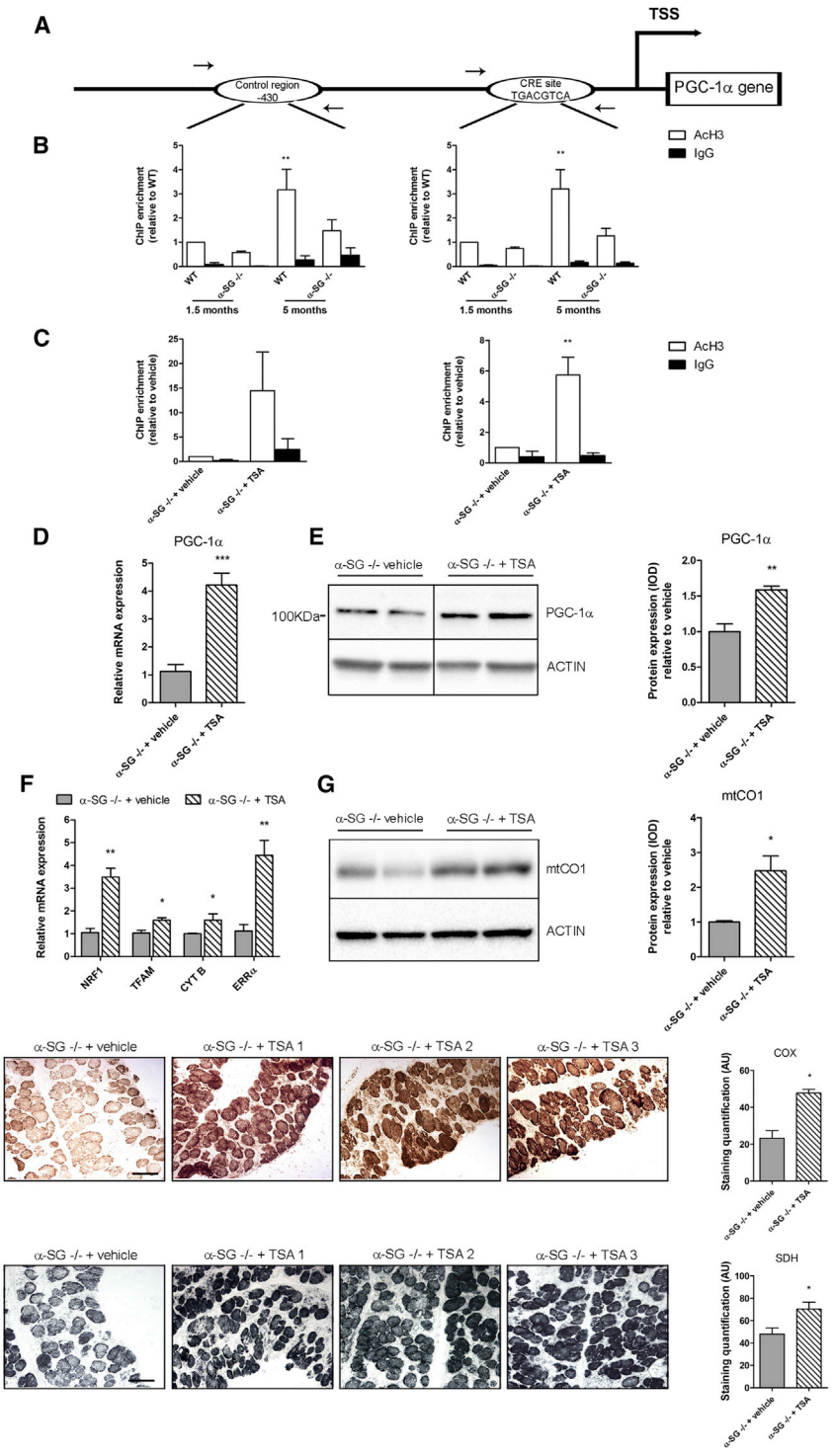

Figure 4. α-SG Null Mice Show Inhibitory Epigenetic Modifications on PGC-1α Promoter Reverted by TSA

(A) Schematic representation of PGC-1α proximal promoter with primers used to amplify TSS-430 and CRE regions.

(B and C) ChIP analysis of PGC-1α proximal promoter performed in diaphragm homogenates at 1.5 and 5 months of age (B) or after TSA treatment (C) (n = 4 per genotype or treatment). Graphs show quantitative PCR values normalized against the input DNA and relative to either WT 1.5 months (B) or vehicle-treated (C) mice (**p < 0.01). AcH3: H3 acetylation; IgG: immunoglobulin.

(D) Quantitative real-time PCR analysis of PGC-1α in diaphragm of α-SG$^{-/-}$ mice after TSA or vehicle treatment (n = 4). *Versus vehicle-treated mice (*p < 0.05, **p < 0.01, ***p < 0.001).

(E) Immunoblot of PGC-1α and actin after TSA or vehicle treatment (n = 4). Densitometric quantification is provided. *Versus vehicle-treated mice (**p < 0.01).

(F) Quantitative real-time PCR analysis of NRF1, TFAM, CYT B, and ERRα genes in diaphragm of α-SG$^{-/-}$ mice after TSA or vehicle treatment (n = 4). *Versus vehicle-treated mice (*p < 0.05, **p < 0.01).

(G) Immunoblot of mtCO1 and actin after TSA or vehicle treatment (n = 4). Densitometric quantification is provided. *Versus vehicle-treated mice (*p < 0.05).

(H and I) Representative COX (H) and SDH (I) staining of vehicle- and TSA-treated diaphragms. Scale bars, 100 μm. Staining quantification (n = 4) is provided. *Versus vehicle-treated mice (*p < 0.05). Values are expressed as mean ± SEM. See also Figure S3.

NO Treatment Induces a SIRT-1-Dependent Shift toward More Oxidative Muscle Fibers

To assess whether SIRT1 activation is required for the induction of fatty acid oxidation and the shift toward more oxidative metabolism induced by NO, α-SG null mice were treated with or without molsidomine for 4 months in the presence or absence, in the last 2 months, of nicotinamide (NAM), a specific SIRT1 inhibitor (Avalos et al., 2005; Green et al., 2008).

NAM administration abolished completely the effect of molsidomine on PGC-1α protein, restoring the acetylation levels to those observed in the untreated α-SG null mice (Figure 7A). In addition, NAM blocked the ability of molsidomine to enhance ADP-driven (state 3) and succinate-stimulated respiratory rates (state 3 + S and state 3 + S + Rot) (Figure 7B). In line with these data, NAM prevented the (NO-dependent) induction of the genes promoting FAO pathway, peroxisome proliferator-activated receptor α (PPARα), PDK4, and LCAD (Figure 7C), as well as the enhancement of AMPK activity (Figure 7D), suggesting that the inhibition of SIRT1 results in the complete loss of the metabolic shift induced by NO.

We conclude from these results that NO improves mitochondrial function and promotes fiber switch in α-SG null mice via a pathway requiring SIRT1 and leading to AMPK activation and FAO.

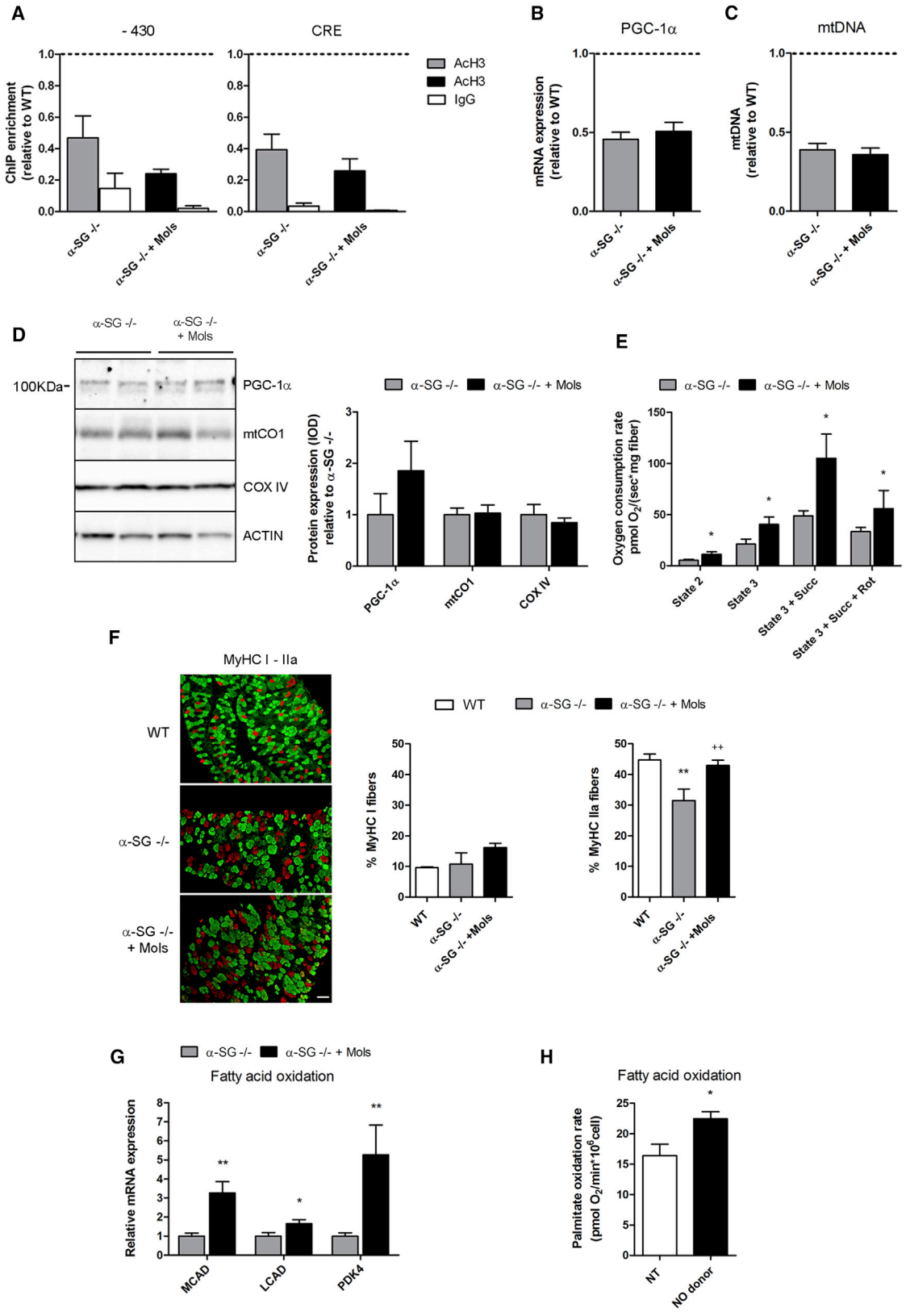

(legend on next page)

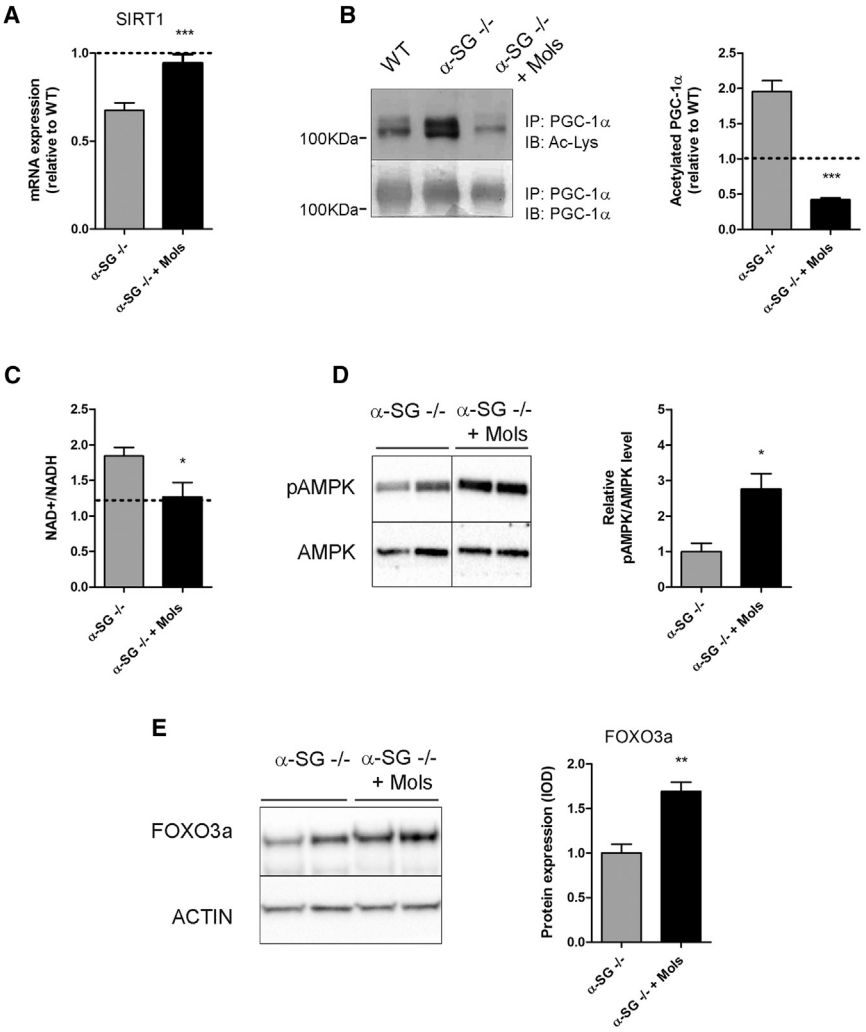

Figure 6. Molsidomine Affects Muscle Metabolism through SIRT1 Modulation and AMPK Activation

Analyses of α-SG$^{-/-}$ diaphragm treated or not with molsidomine.

(A) Quantitative real-time PCR analysis of SIRT1 relative to WT (dashed line) (n ≥ 8 per group).

(B) Protein homogenates immunoprecipitated (IP) with PGC-1α antibody and analyzed by immunoblot (IB) for lysine acetylation levels compared to total protein (n ≥ 8 per group). Densitometric quantification relative to WT (dashed line) is provided.

(C) Determination of NAD^+/NADH ratio (n ≥ 4 per group).

(D) Representative immunoblot for phospho-AMPK (pAMPK) (Thr172) and total AMPK. The graph shows the pAMPK/total AMPK (n = 7 per group). Densitometric quantification is provided.

(E) Representative immunoblot for FOXO3a and actin (n = 4 per group). Densitometric quantification is provided.

Values are expressed as mean ± SEM. *Versus untreated α-SG$^{-/-}$ mice (*p < 0.05, **p < 0.01, ***p < 0.001). See also Figure S6.

DISCUSSION

In this study, we demonstrate a mitochondrial defect in LGMD-2D, and we characterize it functionally and molecularly, providing key information on LGMD-2D pathophysiology and possible strategies for the development of therapeutic approaches.

Defects in mitochondria are emerging as determinant in many muscle disorders (Millay et al., 2008; Ripolone et al., 2015), and some aspects of it have been investigated in muscular dystrophy (Chen et al., 2000; Godin et al., 2012; Guevel et al., 2011; Percival et al., 2013; Pescatori et al., 2007; Rybalka et al., 2014) suggesting that targeting mitochondrial dysfunctions ameliorates the dystrophic phenotype (Millay et al., 2008; Reutenauer et al., 2008). However, no information has been reported yet on the mitochondrial phenotype in the skeletal muscles of LGMD-2D. In the present study, we identify in LGMD-2D a specific mitochondrial deficiency associated with the impairment of the dystrophin-glycoprotein complex and sarcolemmal instability. In LGMD-2D patients, we observed reduced mitochondrial content and expression of key regulators of mitochondrial biogenesis, as well as an impaired OxPhos activity. In the LGMD-2D α-SG null mice, muscles displayed low oxidative metabolism, dependent on reduced levels

Figure 5. NO Donor Molsidomine Modulates Mitochondrial Function without Affecting Mitochondrial Biogenesis

Analyses of α-SG$^{-/-}$ diaphragm treated or not with molsidomine.

(A) ChIP analysis of PGC-1α proximal promoter in diaphragm homogenates. Graphs show quantitative PCR values normalized against the input DNA relative to WT (dashed lines) (n = 4 per group).

(B and C) Quantitative real-time PCR analysis of PGC-1α mRNA (B) and analysis of mtDNA content (C) relative to WT (dashed lines) (n ≥ 4 per group).

(D) Immunoblot of PGC-1α, mtCO1, COX IV, and actin in diaphragm homogenates (n = 4 per group). Densitometric quantification relative to α-SG$^{-/-}$ is provided.

(E) Mitochondrial respiration in permeabilized muscle fibers (n = 6 per group). *Versus untreated α-SG$^{-/-}$ mice (*p < 0.05).

(F) Representative MyHCs immunostaining on diaphragm sections of WT and α-SG$^{-/-}$ mice treated or not with molsidomine. Percentage of MyHC I (red) and MyHC IIa (green) fibers (n ≥ 3 per group). Scale bar, 100 μm. *Versus WT (**p < 0.01); $^+$versus untreated α-SG$^{-/-}$ mice ($^{++}$p < 0.01).

(G) Quantitative real-time PCR analysis of genes of fatty acid oxidation (n ≥ 5 per group).

(H) Palmitate oxidation rate in C2C12 cells treated or not (NT) with NO donor (SIN-1, see the Supplemental Experimental Procedures) (n = 3). *Versus NT (*p < 0.05).

Values are expressed as mean ± SEM. See also Figures S4 and S5.

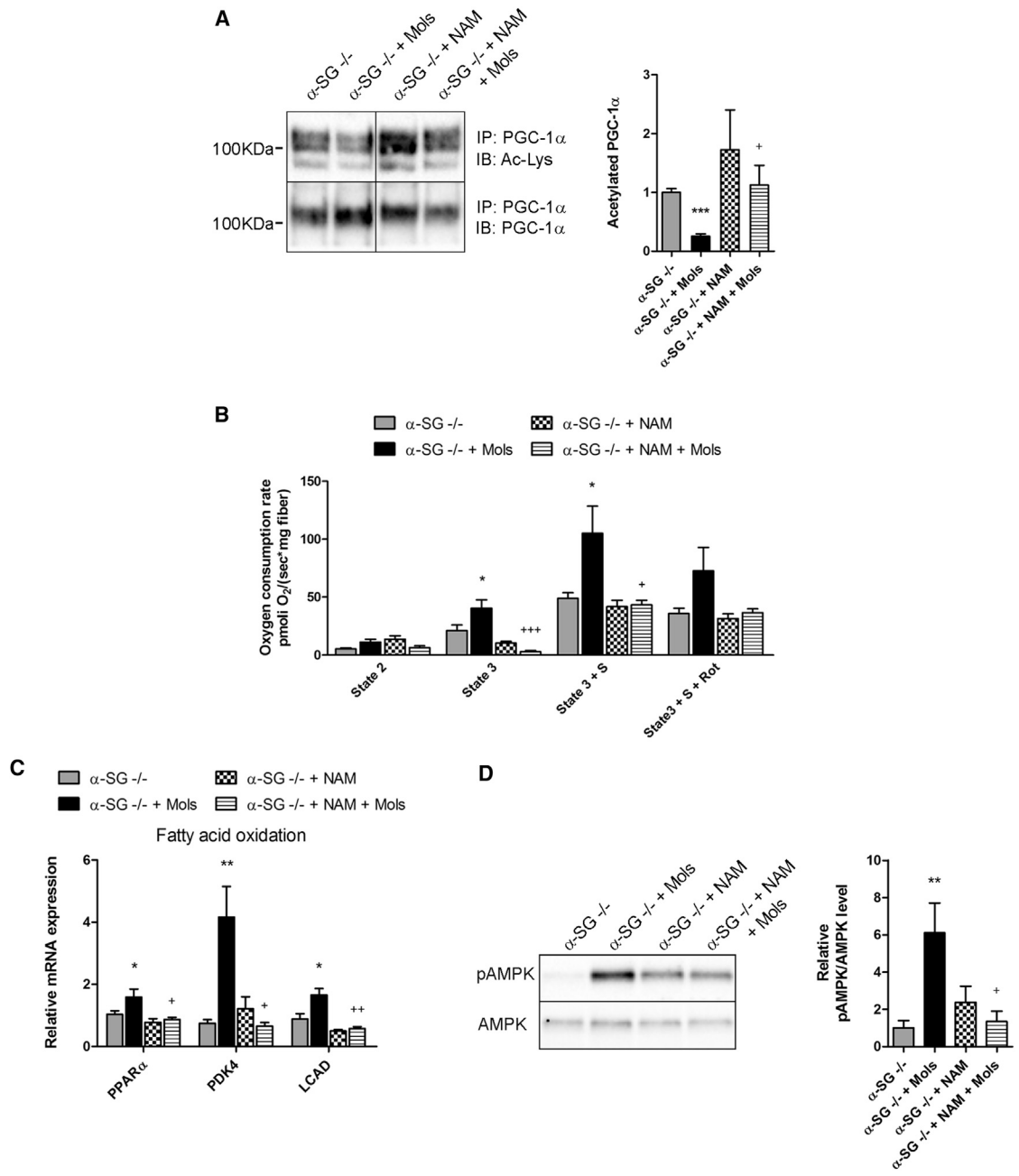

Figure 7. The NO-Induced Shift toward More Oxidative Muscle Fiber Is SIRT1-Dependent

Analyses of α-SG$^{-/-}$ diaphragm treated or not with molsidomine in presence or absence of NAM.

(A) Homogenates were immunoprecipitated (IP) with PGC-1α antibody and analyzed by immunoblot (IB) for lysine acetylation levels compared to total protein (n ≥ 4 per group). Densitometric quantification is provided.

(B) Mitochondrial respiration in permeabilized muscle fibers (n ≥ 4 per group).

(C) Quantitative real-time PCR analysis of genes involved in fatty acid oxidation (n ≥ 4 per group).

(D) Representative immunoblot for phospho-AMPK (pAMPK) (Thr172) and total AMPK. The graph shows the pAMPK/total AMPK (n ≥ 4 per group).

Values are expressed as mean ± SEM. *Versus α-SG$^{-/-}$ mice (*p < 0.05, **p < 0.01, ***p < 0.001); $^{+}$versus α-SG$^{-/-}$ molsidomine-treated mice ($^{+}$p < 0.05, $^{++}$p < 0.01, $^{+++}$p < 0.001).

of PGC-1α and its target genes, leading to a decreased mitochondrial number and reduced slow fiber-type composition. Mitochondrial biogenesis was not induced by classical physiological stimuli including development and cold (Hock and Kralli, 2009; Laker et al., 2012), indicating a persistent and severe defect. This suggests that α-SG null muscles are unable to cope with metabolic

environmental conditions that require mitochondrial biogenesis. Interestingly, in the α-SG null mice, a "mitochondrial crisis" has been observed (Chen et al., 2000), and the low mitochondrial number resulting from the impaired biogenesis process, described here, may be considered the most likely cause.

We next investigated the mechanism responsible for the impairment of the mitochondrial biogenetic pathway. In dystrophic condition, HDACs have an increased activity compared to control, and impaired NO production could contribute to the dysregulation of epigenetic pathways involving HDACs (Colussi et al., 2008, 2009; Illi et al., 2009).

We found that the defective mitochondrial biogenesis depended on epigenetic modifications of the PGC-1α promoter that was characterized by a condensed and repressed chromatin structure. Histone acetylation is a hallmark of active chromatin structure, as it allows chromatin relaxation and efficient gene transcription by reversing the positive charges on histones (Hebbes et al., 1988). We observed that α-SG null muscles exhibit lower levels of H3 acetylation at the PGC-1α promoter. Increased H3 acetylation, by using the panHDACi TSA, could reverse the epigenetic profile (promoter bivalency) at the PGC-1α locus and promote PGC-1α transcription, thereby restoring mitochondrial biogenesis and the oxidative capacity of α-SG null muscles.

Therapeutic approaches modulating PGC-1α expression in muscle have yielded conflicting results. PGC-1α gene transfer in 6-week-old *mdx* mice increases mitochondrial mass (Godin et al., 2012) and *mdx* mice overexpressing PGC-1α selectively in muscle cells show significant induction of OxPhos genes and improved muscle function (Chan et al., 2014). Conversely PGC-1α gene transfer in young (3-week-old) *mdx* mice displays only a relatively modest expression of oxidative genes (Hollinger et al., 2013). These discrepancies may be explained assuming that oxidative response depends on the genetic approach used for PGC-1α manipulation and on the time of induction. Based on our data, we suggest that an alternative therapeutic approach in muscular dystrophy might be the reactivation of the mitochondrial biogenesis by remodeling chromatin structure at the PGC-1α promoter with HDACi drugs, rather than PGC-1α overexpression.

Given the established link between NO and HDAC (Colussi et al., 2008), we tested the efficacy of NO, which has previously shown beneficial effect on dystrophic muscle and on mitochondrial biogenetic activity (Lira et al., 2010; Nisoli et al., 2003, 2007; Tidball and Wehling-Henricks, 2014; Ventura-Clapier et al., 2008). The NO donor molsidomine did not modify the acetylation status of PGC-1α promoter nor the mitochondrial content. Still, NO significantly improved oxidative metabolism and energy expenditure, suggesting the existence of a bioenergetics mechanism, activated by NO, that is able to act as a possible salvage pathway when mitochondrial biogenesis is impaired.

We found that NO enhances fatty acid oxidation and promotes FAO genes transcription, especially PPARα and PPARα target genes, PDK4 and LCAD (Ashmore et al., 2015; Degenhardt et al., 2007; Feige et al., 2008). This drives an oxidative program, which induces a switch toward more oxidative muscle fibers. NO was supplemented with the diet at low concentrations (Sciorati et al., 2011) and its effects could have been due to upregulation of intra-mitochondrial pathways of FAO as it occurs with low/moderate doses of nitrate. In these conditions, nitrates, through NO production, enhance muscle FAO, increasing expression and transcriptional activity of PPARα and β/δ, and driving intra-mitochondrial changes, such as upregulation of malonil-CoA decarboxylase and muscle carnitine concentrations, but without affecting mitochondrial volume (Ashmore et al., 2015).

This phenotype is similar to that described using the SIRT1-specific activator SRT1720, which has a limited activity on mitochondrial density but promotes oxidative metabolism controlling FAO (Feige et al., 2008). Our results indicate that NO acted as SIRT1 activator, and the deacetylation of PGC-1α was the molecular key step leading to activation of PPARα axis and to the oxidative shift, hence SIRT1 and the deacetylation of PGC-1α are essential for NO to increase PGC-1α activity.

SIRT1 activation occurs in low energy conditions such as fasting or calorie restriction (Gerhart-Hines et al., 2007; Rodgers et al., 2005), and SIRT1 activators can, in turn, stimulate pathways associated with low energy status acting as calorie-restriction mimetic (Barger et al., 2008; Feige et al., 2008). Dystrophic mice treated with molsidomine showed high phosphorylation levels of AMPK and an induction of FOXO3a, a specific target of AMPK. However, acute treatment with NO did not directly activate AMPK in myotubes, thus suggesting that NO, via SIRT1, induces key metabolic changes accounting for AMPK activation, which in turn sustains and amplifies FAO. While we cannot exclude possible additional off target actions of molsidomine, our data define NO as a SIRT1 activator that can correct a bioenergetics deficit in dystrophic muscles, ameliorating fatty acid consumption by deacetylation of PGC-1α and induction of metabolic adaptation associated with AMPK activation.

It is important to note that the effect of NO on the activation of SIRT1-PGC-1α pathway persisted over time (20 weeks). This prolonged metabolic action, inducing a therapeutic fiber-type switch, together with the positive effects on the self-renewal ability of satellite cells, inflammatory infiltrate, and fibro-adipogenic precursors cells (Buono et al., 2012; Cordani et al., 2014; Zordan et al., 2013) reinforces the notion that the donation of NO is a valid therapeutic tool for muscular dystrophy.

In view of the importance of reestablishing mitochondrial homeostasis in muscular dystrophy and considering the effect of TSA on mitochondrial biogenesis we describe here, we suggest that a combination of NO with deacetylase inhibitors is an interesting therapeutic option to be explored. This appears of particular relevance for a disease such as LGMD-2D for which corticosteroid therapy is not a valuable tool and other therapies directly addressing the dystrophic muscle are still missing.

EXPERIMENTAL PROCEDURES

Animals Experiments

C57BL/6 α-SG null mice and WT mice were handled in accordance with European Directive (2010/63/UE) and the Italian law on animal care (D.L. 26/2014). The experimental protocols were described in details in the Supplemental Experimental Procedures.

Human Muscle Sample

A total of 11 control and 10 LGMD-2D muscle samples were obtained from the "Biobank of Muscle Tissue, Peripheral Nerve Tissue, DNA, and Cell Lines" of the Neuromuscular and Rare Diseases Unit, Scientific Institute IRCCS

Fondazione Ca' Granda- Ospedale Maggiore Policlinico (Milano, Italy), which is part of the Telethon Genetic Biobank network.

Oxygen Consumption Measurement

Oxygen consumption was measured using Oroboros O_2K oxygraph (Oroboros Instruments) as described in the Supplemental Experimental Procedures.

PGC-1α Acetylation Assay

PGC-1α acetylation was detected by immunoprecipitation in TA and diaphragm muscles as described (Woldt et al., 2013). In brief, muscle tissues were homogenized in a buffer containing 50 mM Tris-HCl (pH 7.4), 68 mM sucrose, 50 mM KCl, 10 mM EDTA, 0.2% BSA, protease, and phosphatase inhibitor mixture. PGC-1α protein was immunoprecipitated from 500 μg of protein homogenate with Santa Cruz antibody against PGC-1α antibody (Santa Cruz Biotechnology, sc-13067, 2 μg per sample) followed by western blot analysis using antibody against acetyl-lysine (1:2,000, Cell Signaling 944, Cell Signaling Technology) and PGC-1α (Cell Signaling 4259). To demonstrate the specificity of the Santa Cruz antibody, we have immunoprecipitated muscle lysate with the Santa Cruz antibody and detected the PGC-1α band with two different antibodies, Cell Signaling 4259 and Millipore, AB3242 (Merck Millipore). The respective IgG as negative control has been used, as shown in the Figure S7.

Chromatin Immunoprecipitation

ChIP assay was performed as previously described (Albini et al., 2013) with minor modifications indicated in the Supplemental Experimental Procedures and using primers specified in Table S2.

Quantitative Real-Time PCR and DNA Quantification

Total RNA and mitochondrial DNA were isolated from human and mouse muscles as described in the Supplemental Experimental Procedures and amplified using the primers listed in Table S1.

Statistical Analysis

Statistical significance of raw data between the groups in each experiment was evaluated using unpaired Student's t test (single comparisons) or one-way ANOVA followed by Bonferroni or Tukey post-tests (multiple comparisons). When data are not normally distributed, the Mann-Whitney test was used and, when indicated, data belonging from different experiments were represented and averaged in the same graph. The GraphPad Prism software package (Graph Software) was used. The results are expressed as means ± SEM of the indicated n values. A probability of <5% ($p < 0.05$) was considered to be significant.

SUPPLEMENTAL INFORMATION

Supplemental Information includes Supplemental Experimental Procedures, seven figures, and two tables and can be found with this article online at http://dx.doi.org/10.1016/j.celrep.2016.11.044.

AUTHORS CONTRIBUTIONS

S.P., M.G., and C.D.P. designed the study, conducted the experiments, and analyzed and interpreted data. C.P., S.Z., D.C., I.D.R., and C.M. performed the experiments and participated to the interpretation of the data. P.L.P and L.L. performed and analyzed ChIP experiments. M.R., R.V., and M.M. supported the acquisition and analysis of human samples. E.C. participated in the design of the study and interpretation of data. C.D.P., C.P., D.C., M.T.B., P.L.P., L.L., and E.C. wrote the final version of the manuscript. All authors read and approved the final manuscript.

ACKNOWLEDGMENTS

The authors thank Elena Vezzoli and Maura Francolini, at Fondazione Filarete (Milano, Italy) for the electron microscopy analysis. We also thank The Italian Association of Myology, Associazione Amici del Centro Dino Ferrari, University of Milan, Eurobiobank, and Telethon network of Genetic biobanks (grant number GTB12001) for providing human biological samples. This work was supported by "Ministero della Salute Giovani Ricercatori GR-2011-02350544" grant to C.D.P.; "Ricerca corrente 2016" and "Ministero dell'Istruzione, Università e Ricerca PRIN2015" grants to E.C.; and "Epigen Project PB. P01.001.019/Progetto Bandiera Epigenomica IFT" grant to L.L.

Received: October 1, 2015
Revised: June 10, 2016
Accepted: November 11, 2016
Published: December 13, 2016

REFERENCES

Albini, S., Coutinho, P., Malecova, B., Giordani, L., Savchenko, A., Forcales, S.V., and Puri, P.L. (2013). Epigenetic reprogramming of human embryonic stem cells into skeletal muscle cells and generation of contractile myospheres. Cell Rep. *3*, 661–670.

Ashmore, T., Roberts, L.D., Morash, A.J., Kotwica, A.O., Finnerty, J., West, J.A., Murfitt, S.A., Fernandez, B.O., Branco, C., Cowburn, A.S., et al. (2015). Nitrate enhances skeletal muscle fatty acid oxidation via a nitric oxide-cGMP-PPAR-mediated mechanism. BMC Biol. *13*, 110.

Avalos, J.L., Bever, K.M., and Wolberger, C. (2005). Mechanism of sirtuin inhibition by nicotinamide: altering the NAD(+) cosubstrate specificity of a Sir2 enzyme. Mol. Cell *17*, 855–868.

Azuara, V., Perry, P., Sauer, S., Spivakov, M., Jørgensen, H.F., John, R.M., Gouti, M., Casanova, M., Warnes, G., Merkenschlager, M., and Fisher, A.G. (2006). Chromatin signatures of pluripotent cell lines. Nat. Cell Biol. *8*, 532–538.

Barger, J.L., Kayo, T., Vann, J.M., Arias, E.B., Wang, J., Hacker, T.A., Wang, Y., Raederstorff, D., Morrow, J.D., Leeuwenburgh, C., et al. (2008). A low dose of dietary resveratrol partially mimics caloric restriction and retards aging parameters in mice. PLoS ONE *3*, e2264.

Barton, E.R., Morris, L., Kawana, M., Bish, L.T., and Toursel, T. (2005). Systemic administration of L-arginine benefits mdx skeletal muscle function. Muscle Nerve *32*, 751–760.

Bernstein, B.E., Mikkelsen, T.S., Xie, X., Kamal, M., Huebert, D.J., Cuff, J., Fry, B., Meissner, A., Wernig, M., Plath, K., et al. (2006). A bivalent chromatin structure marks key developmental genes in embryonic stem cells. Cell *125*, 315–326.

Brunelli, S., Sciorati, C., D'Antona, G., Innocenzi, A., Covarello, D., Galvez, B.G., Perrotta, C., Monopoli, A., Sanvito, F., Bottinelli, R., et al. (2007). Nitric oxide release combined with nonsteroidal antiinflammatory activity prevents muscular dystrophy pathology and enhances stem cell therapy. Proc. Natl. Acad. Sci. USA *104*, 264–269.

Buono, R., Vantaggiato, C., Pisa, V., Azzoni, E., Bassi, M.T., Brunelli, S., Sciorati, C., and Clementi, E. (2012). Nitric oxide sustains long-term skeletal muscle regeneration by regulating fate of satellite cells via signaling pathways requiring Vangl2 and cyclic GMP. Stem Cells *30*, 197–209.

Cacchiarelli, D., Martone, J., Girardi, E., Cesana, M., Incitti, T., Morlando, M., Nicoletti, C., Santini, T., Sthandier, O., Barberi, L., et al. (2010). MicroRNAs involved in molecular circuitries relevant for the Duchenne muscular dystrophy pathogenesis are controlled by the dystrophin/nNOS pathway. Cell Metab. *12*, 341–351.

Chan, M.C., Rowe, G.C., Raghuram, S., Patten, I.S., Farrell, C., and Arany, Z. (2014). Post-natal induction of PGC-1α protects against severe muscle dystrophy independently of utrophin. Skelet. Muscle *4*, 2.

Chen, D., and Guarente, L. (2007). SIR2: a potential target for calorie restriction mimetics. Trends Mol. Med. *13*, 64–71.

Chen, Y.W., Zhao, P., Borup, R., and Hoffman, E.P. (2000). Expression profiling in the muscular dystrophies: identification of novel aspects of molecular pathophysiology. J. Cell Biol. *151*, 1321–1336.

Colussi, C., Mozzetta, C., Gurtner, A., Illi, B., Rosati, J., Straino, S., Ragone, G., Pescatori, M., Zaccagnini, G., Antonini, A., et al. (2008). HDAC2 blockade by nitric oxide and histone deacetylase inhibitors reveals a common target in

Duchenne muscular dystrophy treatment. Proc. Natl. Acad. Sci. USA *105*, 19183–19187.

Colussi, C., Gurtner, A., Rosati, J., Illi, B., Ragone, G., Piaggio, G., Moggio, M., Lamperti, C., D'Angelo, G., Clementi, E., et al. (2009). Nitric oxide deficiency determines global chromatin changes in Duchenne muscular dystrophy. FASEB J. *23*, 2131–2141.

Consalvi, S., Mozzetta, C., Bettica, P., Germani, M., Fiorentini, F., Del Bene, F., Rocchetti, M., Leoni, F., Monzani, V., Mascagni, P., et al. (2013). Preclinical studies in the mdx mouse model of duchenne muscular dystrophy with the histone deacetylase inhibitor givinostat. Mol. Med. *19*, 79–87.

Cordani, N., Pisa, V., Pozzi, L., Sciorati, C., and Clementi, E. (2014). Nitric oxide controls fat deposition in dystrophic skeletal muscle by regulating fibro-adipogenic precursor differentiation. Stem Cells *32*, 874–885.

Crosbie, R.H., Barresi, R., and Campbell, K.P. (2002). Loss of sarcolemma nNOS in sarcoglycan-deficient muscle. FASEB J. *16*, 1786–1791.

D'Angelo, M.G., Gandossini, S., Martinelli Boneschi, F., Sciorati, C., Bonato, S., Brighina, E., Comi, G.P., Turconi, A.C., Magri, F., Stefanoni, G., et al. (2012). Nitric oxide donor and non steroidal anti inflammatory drugs as a therapy for muscular dystrophies: evidence from a safety study with pilot efficacy measures in adult dystrophic patients. Pharmacol. Res. *65*, 472–479.

De Palma, C., and Clementi, E. (2012). Nitric oxide in myogenesis and therapeutic muscle repair. Mol. Neurobiol. *46*, 682–692.

De Palma, C., Falcone, S., Pisoni, S., Cipolat, S., Panzeri, C., Pambianco, S., Pisconti, A., Allevi, R., Bassi, M.T., Cossu, G., et al. (2010). Nitric oxide inhibition of Drp1-mediated mitochondrial fission is critical for myogenic differentiation. Cell Death Differ. *17*, 1684–1696.

Degenhardt, T., Saramäki, A., Malinen, M., Rieck, M., Väisänen, S., Huotari, A., Herzig, K.H., Müller, R., and Carlberg, C. (2007). Three members of the human pyruvate dehydrogenase kinase gene family are direct targets of the peroxisome proliferator-activated receptor beta/delta. J. Mol. Biol. *372*, 341–355.

Feige, J.N., Lagouge, M., Canto, C., Strehle, A., Houten, S.M., Milne, J.C., Lambert, P.D., Mataki, C., Elliott, P.J., and Auwerx, J. (2008). Specific SIRT1 activation mimics low energy levels and protects against diet-induced metabolic disorders by enhancing fat oxidation. Cell Metab. *8*, 347–358.

Galmozzi, A., Mitro, N., Ferrari, A., Gers, E., Gilardi, F., Godio, C., Cermenati, G., Gualerzi, A., Donetti, E., Rotili, D., et al. (2013). Inhibition of class I histone deacetylases unveils a mitochondrial signature and enhances oxidative metabolism in skeletal muscle and adipose tissue. Diabetes *62*, 732–742.

Gerhart-Hines, Z., Rodgers, J.T., Bare, O., Lerin, C., Kim, S.H., Mostoslavsky, R., Alt, F.W., Wu, Z., and Puigserver, P. (2007). Metabolic control of muscle mitochondrial function and fatty acid oxidation through SIRT1/PGC-1alpha. EMBO J. *26*, 1913–1923.

Godin, R., Daussin, F., Matecki, S., Li, T., Petrof, B.J., and Burelle, Y. (2012). Peroxisome proliferator-activated receptor γ coactivator1- gene α transfer restores mitochondrial biomass and improves mitochondrial calcium handling in post-necrotic mdx mouse skeletal muscle. J. Physiol. *590*, 5487–5502.

Green, K.N., Steffan, J.S., Martinez-Coria, H., Sun, X., Schreiber, S.S., Thompson, L.M., and LaFerla, F.M. (2008). Nicotinamide restores cognition in Alzheimer's disease transgenic mice via a mechanism involving sirtuin inhibition and selective reduction of Thr231-phosphotau. J. Neurosci. *28*, 11500–11510.

Guevel, L., Lavoie, J.R., Perez-Iratxeta, C., Rouger, K., Dubreil, L., Feron, M., Talon, S., Brand, M., and Megeney, L.A. (2011). Quantitative proteomic analysis of dystrophic dog muscle. J. Proteome Res. *10*, 2465–2478.

Hebbes, T.R., Thorne, A.W., and Crane-Robinson, C. (1988). A direct link between core histone acetylation and transcriptionally active chromatin. EMBO J. *7*, 1395–1402.

Hock, M.B., and Kralli, A. (2009). Transcriptional control of mitochondrial biogenesis and function. Annu. Rev. Physiol. *71*, 177–203.

Hollinger, K., Gardan-Salmon, D., Santana, C., Rice, D., Snella, E., and Selsby, J.T. (2013). Rescue of dystrophic skeletal muscle by PGC-1α involves restored expression of dystrophin-associated protein complex components and satellite cell signaling. Am. J. Physiol. Regul. Integr. Comp. Physiol. *305*, R13–R23.

Illi, B., Colussi, C., Grasselli, A., Farsetti, A., Capogrossi, M.C., and Gaetano, C. (2009). NO sparks off chromatin: tales of a multifaceted epigenetic regulator. Pharmacol. Ther. *123*, 344–352.

Kornegay, J.N., Spurney, C.F., Nghiem, P.P., Brinkmeyer-Langford, C.L., Hoffman, E.P., and Nagaraju, K. (2014). Pharmacologic management of Duchenne muscular dystrophy: target identification and preclinical trials. ILAR J *55*, 119–149.

Lagouge, M., Argmann, C., Gerhart-Hines, Z., Meziane, H., Lerin, C., Daussin, F., Messadeq, N., Milne, J., Lambert, P., Elliott, P., et al. (2006). Resveratrol improves mitochondrial function and protects against metabolic disease by activating SIRT1 and PGC-1alpha. Cell *127*, 1109–1122.

Laker, R.C., Wadley, G.D., McConell, G.K., and Wlodek, M.E. (2012). Stage of perinatal development regulates skeletal muscle mitochondrial biogenesis and myogenic regulatory factor genes with little impact of growth restriction or cross-fostering. J. Dev. Orig. Health Dis. *3*, 39–51.

Lin, J., Handschin, C., and Spiegelman, B.M. (2005). Metabolic control through the PGC-1 family of transcription coactivators. Cell Metab. *1*, 361–370.

Lira, V.A., Brown, D.L., Lira, A.K., Kavazis, A.N., Soltow, Q.A., Zeanah, E.H., and Criswell, D.S. (2010). Nitric oxide and AMPK cooperatively regulate PGC-1 in skeletal muscle cells. J. Physiol. *588*, 3551–3566.

Mikkelsen, T.S., Ku, M., Jaffe, D.B., Issac, B., Lieberman, E., Giannoukos, G., Alvarez, P., Brockman, W., Kim, T.K., Koche, R.P., et al. (2007). Genome-wide maps of chromatin state in pluripotent and lineage-committed cells. Nature *448*, 553–560.

Millay, D.P., Sargent, M.A., Osinska, H., Baines, C.P., Barton, E.R., Vuagniaux, G., Sweeney, H.L., Robbins, J., and Molkentin, J.D. (2008). Genetic and pharmacologic inhibition of mitochondrial-dependent necrosis attenuates muscular dystrophy. Nat. Med. *14*, 442–447.

Minetti, G.C., Colussi, C., Adami, R., Serra, C., Mozzetta, C., Parente, V., Fortuni, S., Straino, S., Sampaolesi, M., Di Padova, M., et al. (2006). Functional and morphological recovery of dystrophic muscles in mice treated with deacetylase inhibitors. Nat. Med. *12*, 1147–1150.

Nisoli, E., Clementi, E., Paolucci, C., Cozzi, V., Tonello, C., Sciorati, C., Bracale, R., Valerio, A., Francolini, M., Moncada, S., and Carruba, M.O. (2003). Mitochondrial biogenesis in mammals: the role of endogenous nitric oxide. Science *299*, 896–899.

Nisoli, E., Clementi, E., Carruba, M.O., and Moncada, S. (2007). Defective mitochondrial biogenesis: a hallmark of the high cardiovascular risk in the metabolic syndrome? Circ. Res. *100*, 795–806.

Percival, J.M., Siegel, M.P., Knowels, G., and Marcinek, D.J. (2013). Defects in mitochondrial localization and ATP synthesis in the mdx mouse model of Duchenne muscular dystrophy are not alleviated by PDE5 inhibition. Hum. Mol. Genet. *22*, 153–167.

Pescatori, M., Broccolini, A., Minetti, C., Bertini, E., Bruno, C., D'amico, A., Bernardini, C., Mirabella, M., Silvestri, G., Giglio, V., et al. (2007). Gene expression profiling in the early phases of DMD: a constant molecular signature characterizes DMD muscle from early postnatal life throughout disease progression. FASEB J. *21*, 1210–1226.

Reutenauer, J., Dorchies, O.M., Patthey-Vuadens, O., Vuagniaux, G., and Ruegg, U.T. (2008). Investigation of Debio 025, a cyclophilin inhibitor, in the dystrophic mdx mouse, a model for Duchenne muscular dystrophy. Br. J. Pharmacol. *155*, 574–584.

Ripolone, M., Ronchi, D., Violano, R., Vallejo, D., Fagiolari, G., Barca, E., Lucchini, V., Colombo, I., Villa, L., Berardinelli, A., et al. (2015). Impaired muscle mitochondrial biogenesis and myogenesis in spinal muscular atrophy. JAMA Neurol. *72*, 666–675.

Rodgers, J.T., Lerin, C., Haas, W., Gygi, S.P., Spiegelman, B.M., and Puigserver, P. (2005). Nutrient control of glucose homeostasis through a complex of PGC-1alpha and SIRT1. Nature *434*, 113–118.

Ruegg, U.T. (2013). Pharmacological prospects in the treatment of Duchenne muscular dystrophy. Curr. Opin. Neurol. *26*, 577–584.

Rybalka, E., Timpani, C.A., Cooke, M.B., Williams, A.D., and Hayes, A. (2014). Defects in mitochondrial ATP synthesis in dystrophin-deficient mdx skeletal muscles may be caused by complex I insufficiency. PLoS ONE *9*, e115763.

Sciorati, C., Buono, R., Azzoni, E., Casati, S., Ciuffreda, P., D'Angelo, G., Cattaneo, D., Brunelli, S., and Clementi, E. (2010). Co-administration of ibuprofen and nitric oxide is an effective experimental therapy for muscular dystrophy, with immediate applicability to humans. Br. J. Pharmacol. *160*, 1550–1560.

Sciorati, C., Miglietta, D., Buono, R., Pisa, V., Cattaneo, D., Azzoni, E., Brunelli, S., and Clementi, E. (2011). A dual acting compound releasing nitric oxide (NO) and ibuprofen, NCX 320, shows significant therapeutic effects in a mouse model of muscular dystrophy. Pharmacol. Res. *64*, 210–217.

Stamler, J.S., and Meissner, G. (2001). Physiology of nitric oxide in skeletal muscle. Physiol. Rev. *81*, 209–237.

Summermatter, S., Thurnheer, R., Santos, G., Mosca, B., Baum, O., Treves, S., Hoppeler, H., Zorzato, F., and Handschin, C. (2012). Remodeling of calcium handling in skeletal muscle through PGC-1α: impact on force, fatigability, and fiber type. Am. J. Physiol. Cell Physiol. *302*, C88–C99.

Tidball, J.G., and Wehling-Henricks, M. (2014). Nitric oxide synthase deficiency and the pathophysiology of muscular dystrophy. J. Physiol. *592*, 4627–4638.

Ventura-Clapier, R., Garnier, A., and Veksler, V. (2008). Transcriptional control of mitochondrial biogenesis: the central role of PGC-1alpha. Cardiovasc. Res. *79*, 208–217.

Woldt, E., Sebti, Y., Solt, L.A., Duhem, C., Lancel, S., Eeckhoute, J., Hesselink, M.K., Paquet, C., Delhaye, S., Shin, Y., et al. (2013). Rev-erb-α modulates skeletal muscle oxidative capacity by regulating mitochondrial biogenesis and autophagy. Nat. Med. *19*, 1039–1046.

Zordan, P., Sciorati, C., Campana, L., Cottone, L., Clementi, E., Querini, P.R., and Brunelli, S. (2013). The nitric oxide-donor molsidomine modulates the innate inflammatory response in a mouse model of muscular dystrophy. Eur. J. Pharmacol. *715*, 296–303.